

Surface-Enhanced Raman Scattering (SERS) and Surface-Enhanced Fluorescence (SEF) in the context of modified spontaneous emission

E. C. Le Ru* and P. G. Etchegoin†

The MacDiarmid Institute for Advanced Materials and Nanotechnology, School of Chemical and Physical Sciences, Victoria University of Wellington, PO Box 600, Wellington, New Zealand‡

(Dated: August 21, 2018)

Surface Enhanced Raman Scattering (SERS) and Surface-Enhanced Fluorescence (SEF) are studied within the framework of modified Spontaneous Emission (SE), and similarities and differences are highlighted. This description sheds new light into several aspects of the SERS electromagnetic enhancement. In addition, combined with the optical reciprocity theorem it also provides a rigorous justification of a generalized version of the widely used SERS enhancement factor proportional to the fourth power of the field ($|E|^4$). We show, in addition, that this approach also applies to the calculation of Surface-Enhanced Fluorescence cross-sections thus presenting both phenomena SERS and SEF within a unified framework.

PACS numbers: 33.20.Fb, 33.50.-j, 78.67.Bf, 87.64.Je

Keywords: Surface Enhanced Raman Scattering, SERS, Spontaneous emission, modified spontaneous emission, Surface Enhanced Fluorescence, Metal-Enhanced Fluorescence, Surface plasmon, Mie theory, quantum yield, fluorescence quenching, Optical Reciprocity Theorem, Vibrational pumping

I. INTRODUCTION

The emission properties of a dipole are affected by its environment. This fact was first pointed out by Purcell [1] and has since then been demonstrated experimentally in a wide range of experimental situations; for example for excited Eu^{3+} ions in front of a plane metallic surface, as in the original observation by Drexhage [2], or for Rydberg atoms in an optical cavity [3]. This effect can be particularly strong in close proximity of metallic structures [4, 5, 6]. It is evident in the modification (quenching or enhancement) of spontaneous emission (SE) rates [7]. Although this effect has been assumed for some time to lead to a strong quenching of the fluorescence, instances of enhanced fluorescence have been reported more recently for dyes [8], and even for quantum dots [9], so-called Surface-Enhanced Fluorescence (SEF) or Metal-Enhanced Fluorescence (MEF). Such enhancements have been known for some time and are even more spectacular in Surface Enhanced Raman Scattering (SERS) [10]. SERS has regained interest lately following the observation of single molecules [11, 12], and possible applications in biology/analytical chemistry [13, 14] and nano-plasmonics [15]. SERS enhancement factors as large as 10^{15} have been reported and are believed to be mainly electromagnetic (EM) in origin, although the detailed mechanism is still debated. It is widely accepted that localized surface plasmon resonances give rise to places with large local field enhancement factors $|E_{\text{Loc}}/E_0|$; so-called hot-spots. In most cases the SERS signal is assumed to be proportional to the power of 4 of this factor [14, 16, 17]: a power of two accounting for the excitation part, and a power of

two for the emission. This assumption, although widely used in particular to explain the enhancements required for single molecule SERS, has never been rigorously justified, as we shall show in the forthcoming discussion.

Numerous theoretical studies have concentrated on the modification of SE rates inside dielectric materials, perfect or absorbing, and close to boundaries with dielectrics or metals. Optical cavities, and similarly photonic crystals, can also strongly enhance, suppress, or redirect the SE field of an atom [3]. Most available results in the literature relate to SE rates in simple geometries such as plane boundaries, spheres, or ellipsoids. Only recently, methods have been proposed for SE rates in more complex nano-structures [18]. Scattering processes (elastic or inelastic) by an atom are in many ways similar to spontaneous emission. Excluding stimulated processes, the scattering of a photon by an atom involves the ‘spontaneous’ creation of a photon in a mode where no photon existed before. One therefore expects a modification of the scattering cross-section in a similar way as SE rates are modified by the environment. The difference between these two processes only lies in the initial state, to wit: excited atom with no photon for SE, or atom in ground state with one incident photon for the case of scattering. Fluorescence is also in many respects similar to scattering. The crucial difference is that scattering is instantaneous while fluorescence is a stepwise process involving absorption, energy relaxation, and spontaneous emission.

It is one of the purposes of this paper to highlight the similarities, and discuss the differences between SE, SEF, and SERS for atoms or molecules in close proximity of metal surfaces. These aspects have been discussed in reviews, in the past [4, 5, 6] and more recently [8], but usually focusing on one specific process. The emphasis will be put, therefore, on the relationships between these processes presenting them under one single framework in a more modern context. In particular, the various methods for calculating SE rates and cross sections, some of them

*Electronic address: Eric.LeRu@vuw.ac.nz

†Electronic address: Pablo.Etchegoin@vuw.ac.nz

‡<http://www.vuw.ac.nz/Raman>

common and others more novel, are described in detail. The description is kept as simple as possible to emphasize the physical aspects. For this reason, we constrain our description to classical electrodynamics with a local dielectric function. We also use isotropic polarizabilities whenever necessary to avoid complicated tensorial notations. The results are illustrated by simple examples of emitters close to a silver sphere. The main advantage is that it does not rely on any approximation for the solution of the electromagnetic problem, since analytic expressions (not discussed here) can be obtained from Mie theory [19]. These choices do not affect the generality of the results and the methods described here can be used for complex geometries provided that a suitable method—usually numerical—is available to solve the electromagnetic problem.

Finally, particular emphasis will also be given to the EM enhancements in SERS. We derive a general formula for the SERS cross sections in the framework of modified SE rates. It highlights the importance of non-radiative vs. radiative enhancements and also emphasizes the strong similarities between SERS enhancement and enhanced SE which, by the same token, requires to reconsider the origin of the fluorescence quenching under SERS conditions. In addition, the optical reciprocity theorem [20] is used to show that these results are consistent with a generalized version of the commonly used $|E|^4$ factor in SERS, with certain (generally overlooked) limitations.

The paper is organized as follows: in Sec. II, we discuss modified SE rates and the various ways of calculating them. In particular, we highlight the use of the optical reciprocity theorem as a method for calculating SE rates, a technique that has not received the attention it should deserve. The modification of the quantum yield of a fluorophore is also discussed. In Sec. III, we apply these arguments to the determination of SERS cross-section. We use the reciprocity theorem to derive a generalized version of the common $|E|^4$ enhancement factor, and show a simple example where this factor would lead to erroneous results. Similar arguments are applied to obtain a simple description of SEF. It is shown that fluorescence quenching or enhancement are usually both possible, depending on the relative contribution of two competing mechanisms, namely: absorption cross-section enhancement and non-radiative quenching. Finally in Sec. IV, we discuss the differences and similarities between SE rates and SERS cross sections. Some common aspects of SERS, such as fluorescence quenching or the presence of an inelastic continuum, and other outstanding issues (such as vibrational pumping) are revisited within this new approach.

II. MODIFIED SPONTANEOUS EMISSION

Spontaneous emission is an intrinsically quantum effect, where a dipolar atomic transition couples to the

vacuum state of the electromagnetic field. This coupling can only occur with the quantized electromagnetic field, where the vacuum state has a zero-point energy and exhibit quantum fluctuations. However, because of the difficulties in the quantization of the field in complex structures, the modification of SE rates is most often studied within a semi-classical model of an oscillating electromagnetic dipole [4]. This leads to results in agreement (in most cases) with experiments and with the full quantum mechanical treatment when possible. Several complementary techniques can also be used; the first of which considers the self-reaction field and is closest to the quantum treatment (and can be shown to be formally equivalent in most cases). The latter enables the derivation of a decay rate but does not distinguish between radiative and non-radiative processes. To avoid this problem, one can use a second technique based on the Poynting vector, which emphasizes energy conservation. We review here the derivation and main results of these two methods. We then describe a third approach, which has hardly been used in the past, but will be important in connection with the SERS cross sections.

SI units are used throughout the paper. Results from these three approaches are illustrated by considering a dipolar emitter at a short distance $d = 1$ or 2 nm from the surface of a silver sphere. Standard Mie theory [19, 21, 22] was used to derive these results, and the environment is assumed to be vacuum ($\epsilon_r = 1$). The (local) wavelength-dependent relative dielectric function of silver was approximated by:

$$\epsilon(\lambda) = \epsilon_\infty - \frac{1}{\lambda_p^2 \left(\frac{1}{\lambda^2} + \frac{i}{\Gamma\lambda} \right)}, \quad (1)$$

where $\epsilon_\infty = 4$, $\lambda_p = 141$ nm, $\Gamma = 17000$ nm. These parameters provide the best Drude fit for the real optical properties of Ag.

A. Spontaneous Emission and self-reaction

Within the classical treatment, SE can be seen as an effect of the self-reaction, i.e. the electromagnetic field \mathbf{E}_{SR} created at the dipole position by itself, either directly or through its interaction with the environment (reflected field). We consider a dipole $\mathbf{d} = d\mathbf{e}_d$, oscillating at a frequency ω (an $e^{-i\omega t}$ dependence is assumed for the fields). The self-reaction field can be written as $\mathbf{E}_{\text{SR}} = \mathbf{G}(\omega)\mathbf{d}$, where $\mathbf{G}(\omega)$ can be viewed as the *self-reaction Green's tensor*, obtained by solving Maxwell's equation with the appropriate boundary conditions.

The SE rate can then be calculated from [18, 23]

$$\Gamma = \frac{2}{\hbar} d^2 \text{Im}(\mathbf{e}_d \mathbf{G}(\omega) \mathbf{e}_d), \quad (2)$$

which can be derived from *quantum* arguments [23]. The parameter d should be taken to be the dipole moment of the transition $d_{\text{qu}}^2 = |-e \langle b | \mathbf{r} \cdot \mathbf{e}_d | a \rangle|^2$, between excited

ment, can be used to calculate the absolute decay rate, Γ or Γ_0 , as in Eq. (4). The Poynting vector approach, however, only yields the relative decay rate (enhancement factor), Γ/Γ_0 . This is not a limitation here, since we are interested precisely in this decay rate enhancement.

Besides, the Poynting vector approach also yields additional information, namely: the non-radiative decay, the radiated power, and its angular dependence (radiation pattern) [4, 18]. In the situation of Fig. 1, where the dipole environment is bounded, one can enclose the emitter and all absorbing media in a large sphere, C_{Rad} , and calculate the power outflow on this surface, which corresponds to the power radiated by the source in the far-field, P_{Rad} . Moreover, if this surface is sufficiently far from any objects and sources, such that the lines of the Poynting vector are approximately radial (radiation field), then one can also obtain $dP_{\text{rad}}/d\Omega(\theta, \phi) = r^2 \text{Re}(\mathbf{S} \cdot \mathbf{e}_r)$, i.e the power radiated per unit solid angle, and deduce the angular radiation pattern. Finally, from the solution of the EM field inside the absorbing media, it is also possible to calculate the total absorbed power, P_{NR} , which corresponds to non-radiative losses. Alternatively, one can also use energy conservation, which ensures that $P_{\text{Tot}} = P_{\text{Rad}} + P_{\text{NR}}$, to obtain the absorbed power from the other two magnitudes.

This technique therefore enables us to calculate the radiative enhancement $M_{\text{Rad}} = P_{\text{Rad}}/P_0$, and the radiative efficiency $\eta_{\text{Rad}} = P_{\text{Rad}}/P_{\text{Tot}}$. These two quantities can also be defined and calculated as a function of angle (θ, ϕ) . It is interesting to note that a large radiative enhancement can coexist with a small radiative efficiency, and vice-versa, depending on the weight of non-radiative processes. What is measured in experiments is usually either the *radiative* SE enhancement M_{Rad} , or the *angle dependent radiative* enhancement $M_{\text{Rad}}(\theta, \phi)$. The *total* SE rate enhancement or decay rate M_{Tot} (radiative+non-radiative) can only be measured in time-resolved experiments.

C. Some simple examples

The problem of an emitter close to a metal surface has been studied extensively in the simple case of a plane surface with various degrees of refinement [4, 26, 27, 28, 29, 30]. Few studies have, however, focused on the regime of small distances between emitter and metal (a few nanometers). In principle, the non-local description of the dielectric function fails at such small distances. However, because of the difficulties of solving the non-local EM problem in complex structures, it is useful to consider the local problem to obtain qualitative and semi-quantitative results. Close to a plane, M_{Tot} can be very large, for example of the order of 10^6 at the Surface Plasmon (SP) resonance ($\text{Re}(\epsilon_r) \approx -1$) of noble metals. However, the radiative enhancement is then (at best) of order ~ 1 , sometimes much smaller. Most of the energy is therefore emitted into non-radiative modes,

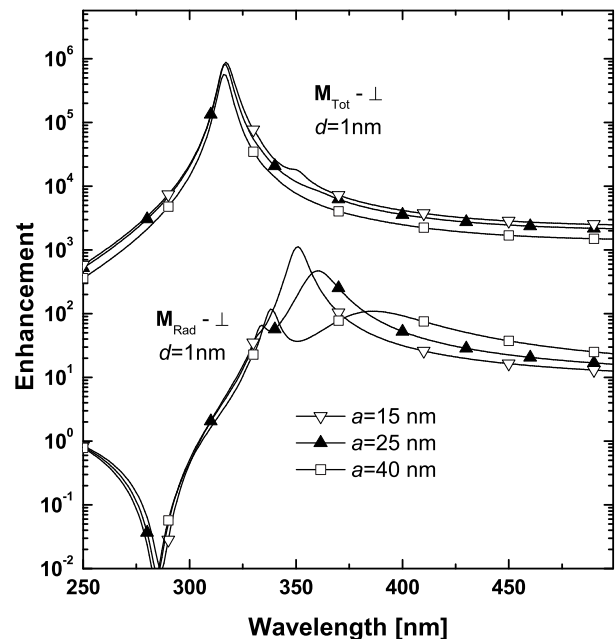


FIG. 2: Total (M_{Tot}) and radiative (M_{Rad}) SE rate enhancements for a dipole perpendicular (at a distance $d = 1$ nm) to silver spheres of radii $a = 15, 25$ and 40 nm. This illustrates the influence of surface plasmon resonances. The peak in M_{Rad} red-shifts with increasing a and corresponds to the surface plasmon resonance of the sphere, which is geometry-dependent. Note also that enhancements are larger at resonance for the smallest spheres. The peak in M_{Tot} does not change with a and remains at 315 nm. This corresponds to the condition $\text{Re}(\epsilon) \approx -1$ and is the intrinsic surface plasmon resonance of a plane silver surface. As can be seen in the plots, this resonance is strongly non-radiative, while the sphere resonance is radiative in essence.

and is eventually dissipated in the metal. These modes have been shown to correspond to non-radiative Surface Plasmon Waves (SPW). Although this identification requires a non-local treatment, the study of the relative contribution of radiative vs non-radiative decays is already contained in the local approximation; this is precisely what is important for the study of processes such as SE, SEF, and SERS. These studies on plane metallic surfaces are the origin of the common belief that fluorescence is always quenched close to metals. We will show here that more complex metallic structures, in particular nano-particles, can lead to enhancements with a large radiative component.

To understand this, we show in Fig. 2 the wavelength dependence of M_{Tot} and M_{Rad} for a dipole perpendicular to the surface of a silver (Ag) sphere. The results are shown for three sizes of spheres with radii $a = 15, 25$, and 40 nm, respectively; typical for colloidal Ag. Varying the radius enables to understand the role of the main dipolar surface plasmon resonance of the sphere, which red-shifts from about 350 to 380 nm as the size increases. M_{Rad} clearly exhibits maxima at the SP resonances. On

the opposite, M_{Tot} remains virtually unchanged for all sizes, peaking at 315 nm ($\text{Re}(\epsilon_r) \approx -1$), corresponding to the intrinsic SP resonance of a plane Ag surface. This can be understood simply: the sphere SP resonance is radiative, and leads to a larger M_{Rad} when the dipole couples to it efficiently. This resonance is strongly *geometry dependent*, and is red-shifted for larger objects, or for coupled objects such as two closely-spaced spheres. However, the intrinsic Ag SP resonance at 315 nm is always strongly non-radiative. It is related to the strong reflected field created by the dipole image. This is *independent of geometry* because the surface is approximately a plane when viewed from the dipole at very short distances. The intensity of the reflected field is however strongly dependent on the distance d of the dipole from the surface, and decreases as d^{-3} . This interpretation is further confirmed in Fig. 3 where the results for two distances, $d = 1$ and 2 nm, are compared. The expected dependence of M_{Tot} with distance is clearly observed, while M_{Rad} remains virtually unchanged. This reflects the fact that M_{Tot} is dominated by the dipole image reflected field (strongly distance dependent), while M_{Rad} depends primarily on how well the dipole emission couples to the radiative SP resonance of the sphere. This coupling is not strongly sensitive to distance, but should however be sensitive to the dipole orientation. This is also illustrated in Fig. 3 where perpendicular and parallel dipoles are compared.

Finally, we can also identify from Figs. 2 and 3 the situations where the radiative enhancement is the largest. First, dipoles perpendicular to the surface present larger enhancements than those parallel to it. Moreover, as already pointed out, M_{Rad} is maximum at the SP resonance of the sphere, which is size-dependent. At this maximum, M_{Rad} is largest for the smallest sphere, with values of ≈ 1100 for $a = 15$ nm, down to ≈ 470 for $a = 25$ nm and ≈ 120 for $a = 40$ nm. For a given radius, M_{Rad} varies little with d , down to ≈ 380 for $d = 2$ nm, or ≈ 210 for $d = 5$ nm (for $a = 25$ nm). However, because M_{Tot} decreases strongly, the radiative efficiency $\eta_{\text{Rad}} = M_{\text{Rad}}/M_{\text{Tot}}$ increases dramatically, from $\eta \approx 0.06$ for $d = 1$ nm to $\eta \approx 0.5$ for $d = 5$ nm.

The previous discussion about metal spheres can be generalized to more complex structures. However, to be quantitative, the solution of the EM problem usually requires some approximations or the use of numerical methods, which are outside the scope of this paper. It is expected that suitable structures could lead to radiative enhancements much larger than those for a sphere. For example, in a recent study [18], numerical methods and the Poynting vector approach were applied to closely spaced gold nano-particles. Values of M_{Rad} up to 2×10^5 were calculated for a dipole placed at a junction between two nano-particles. Here we are sacrificing examples with larger enhancements for the convenience of having an analytic solution to the problem through Mie theory.

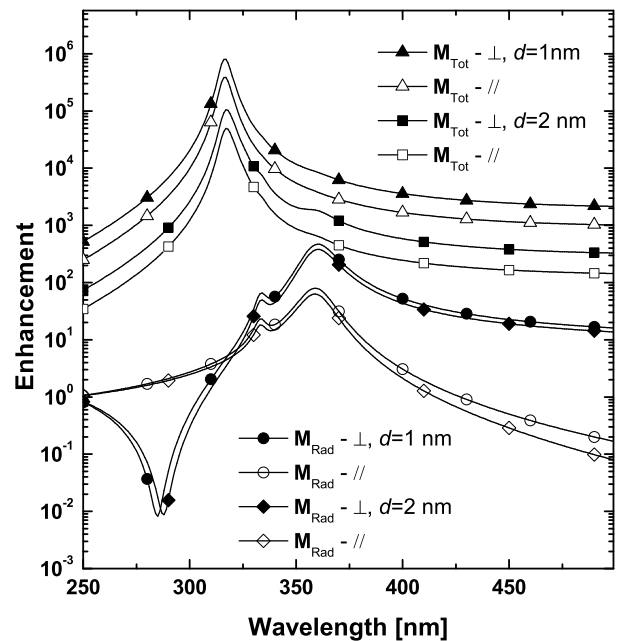


FIG. 3: Total (M_{Tot}) and radiative (M_{Rad}) SE rate enhancements for a dipole close to a silver sphere of radius $a = 25$ nm, as a function of wavelength. The results are shown for dipoles either perpendicular or parallel to the sphere surface, and at a distance $d = 1$ or 2 nm. The total rate enhancements are strongly increased as the dipole gets closer to the surface, while the radiative enhancements do not change much. These plots were obtained using an extension of Mie theory, following Ref. [22]. M_{Rad} is obtained from the Poynting vector approach, and M_{Tot} from the self-reaction approach. See the text for further details.

D. Using the Reciprocity Theorem

The two previous approaches require to solve Maxwell's equations for the dipolar singularity in the presence of boundaries, either numerically or analytically. This can present some problems. Analytically, the dipolar singularity can significantly complicate the problem (for example for a dipole near a sphere [22]). Numerically, singularities are not always straightforward to introduce. An additional inconvenience is that the problem needs to be solved for each dipolar position and orientation that one wants to study. We introduce here a third approach, based on the optical reciprocity theorem, which can circumvent some of these problems. The optical reciprocity theorem (ORT) states [20] that the field \mathbf{E} created at a given point M by a dipole \mathbf{d} (at point O) is related to the field \mathbf{E}_2 at O created by a dipole \mathbf{d}_2 at M according to $\mathbf{d} \cdot \mathbf{E}_2 = \mathbf{d}_2 \cdot \mathbf{E}$. The validity is very general, and in particular in the presence of absorbing dielectrics or metals (assuming a local dielectric function). We show here that this enables to derive the far-field properties of the emitter in a given direction from the solution of two Plane Wave Excitation (PWE) problems, without any source singularities.

We consider our dipole \mathbf{d} at O in Fig. 1, and focus on its far-field emission at a distance R in direction \mathbf{e}_r defined by angles (θ, ϕ) . The radiation field is transverse (no radial component) and can be decomposed into two components, E_θ and E_ϕ , along unit vectors \mathbf{e}_θ and \mathbf{e}_ϕ . The Poynting vector is $\mathbf{S} = (\epsilon_0 c/2)|E|^2 \mathbf{e}_r$. To apply the ORT, we consider first the problem of a dipole $\mathbf{d}_2 = d_0 \mathbf{e}_\theta$ situated in M. The ORT yields $d_0 E_\theta = \mathbf{d} \cdot \mathbf{E}_2$, where \mathbf{E}_2 is the field created by \mathbf{d}_2 at O. For sufficiently large R , the field of this dipole in the region of interest can be approximated by a plane wave propagating along $-\mathbf{e}_r$, polarized along \mathbf{e}_θ , and with amplitude $E_P = k^2 d_0 \exp(ikR)/(4\pi\epsilon_0 R)$. We can now choose d_0 so that $E_P = E_0$. The problem therefore reduces to solving Maxwell's equation for excitation with a plane wave polarized along \mathbf{e}_θ , propagating along $-\mathbf{e}_r$, and of amplitude E_0 . We denote $\mathbf{E}^{\text{PW}-\theta}$ the field at O for this plane wave problem and the ORT then yields for the θ component of the radiation field of \mathbf{d} at M:

$$E_\theta = \frac{k^2 e^{ikR}}{4\pi\epsilon_0 R |E_0|} \mathbf{d} \cdot \mathbf{E}^{\text{PW}-\theta}, \quad (7)$$

A similar expression is obtained for E_ϕ , but note that it requires the solution of a *different PWE problem* with polarization along \mathbf{e}_ϕ . The time-averaged power radiated per unit solid angle is then

$$\frac{dP_{\text{Rad}}}{d\Omega}(\theta, \phi) = R^2 \text{Re}(\mathbf{S} \cdot \mathbf{e}_r) = \frac{R^2 \epsilon_0 c}{2} |E|^2 \quad (8)$$

$$= \frac{\omega^4 d^2}{32\pi^2 \epsilon_0 c^3 |E_0|^2} [|\mathbf{e}_d \cdot \mathbf{E}^{\text{PW}-\theta}|^2 + |\mathbf{e}_d \cdot \mathbf{E}^{\text{PW}-\phi}|^2]. \quad (9)$$

It is easy to verify that the above expression is fully consistent with that of an isolated dipole in free-space, yielding the same expression as from a standard approach [25]. We can therefore write the angle-dependent radiative enhancement as

$$M_{\text{Rad}}(\theta, \phi) = \frac{|\mathbf{e}_d \cdot \mathbf{E}^{\text{PW}-\theta}|^2}{|E_0|^2} + \frac{|\mathbf{e}_d \cdot \mathbf{E}^{\text{PW}-\phi}|^2}{|E_0|^2}, \quad (10)$$

where $\mathbf{E}^{\text{PW}-\theta}$ and $\mathbf{E}^{\text{PW}-\phi}$ can be obtained from the solution of two different PWE problems. The important result to highlight here is that *the radiative property in a given direction of a dipole in a complex environment can be obtained by modelling two PWE problems, without a dipolar singularity*. Eq. (10) shows that the far-field emission of a dipole in a given direction is in some way related to the local field enhancement factor $M_{\text{Loc}} = |E|^2/|E_0|^2$ for PWE from this direction. This will be the basis for a the generalization of the $|E|^4$ SERS enhancement in the next section.

We illustrate the use of the ORT approach in Fig. 4. The angle dependent radiative enhancement in direction $-\mathbf{e}_z$ is calculated for dipoles located at point A (see inset) with 3 different orientations. The results are compared to calculations of the local field enhancement factor $M_{\text{Loc}} = |E|^2/|E_0|^2$ for PWE along \mathbf{e}_z . Local field

and radiative enhancements are nearly identical for a perpendicular dipole, but clearly differ for other orientations. This highlights the difficulties of using purely a local field enhancement approach to the problem of radiative enhancement. The two approaches can be reconciled by the application of the ORT as given in Eq. (10).

We conclude this section with a few remarks:

- In principle, it is also possible within this approach to obtain the total radiative enhancement M_{Rad} by integrating $M_{\text{Rad}}(\theta, \phi)$. However, it is often not practical and the Poynting vector approach is usually better suited for this.
- This approach, contrary to the previous two, yields no information on the total decay enhancement M_{Tot} or decay to non-radiative modes.
- This approach has hardly been used in the past [31], but is actually well suited to many experimental situations where only radiative properties are of interest and where detection is performed in only one direction. We shall come back to it when discussing SERS cross sections.
- We would like to stress that the ORT as stated above does not have, to our knowledge, any direct physical meaning. Its expression, $\mathbf{d} \cdot \mathbf{E}_2 = \mathbf{d}_2 \cdot \mathbf{E}$, looks like a statement about interaction energies between the two dipoles. However, one would need the complex conjugates of the fields (or the dipoles) to be able to translate this in a statement about the interaction energy of each dipole with the field of the other. The demonstration of the ORT [20] does not involve, in fact, the interaction energy. Moreover, the ORT considers the solution of two independent problems with a single dipole and not the problem of the two dipoles at the same time, thus avoiding mutual self-reactions. For these reasons, the ORT has to be viewed as mathematical symmetry relation embedded in Maxwell's equations, which relates the field solution of two independent electromagnetic problems.

E. Quantum yield of a fluorophore

Many applications make use of fluorophores, sometimes in complex environments. There are two important characteristics of a fluorophore: its absorption cross-section and its quantum yield, both of which can be modified by the environment. Using the previous arguments, we focus here on the modified quantum yield. The absorption cross-section will be discussed later in the context of Surface-Enhanced Fluorescence (SEF).

The fluorescence quantum yield is the proportion of the population of excited electrons that decay radiatively to the ground state, hence producing a detectable photon. It is related to the radiative decay rate Γ_{Rad} , but other

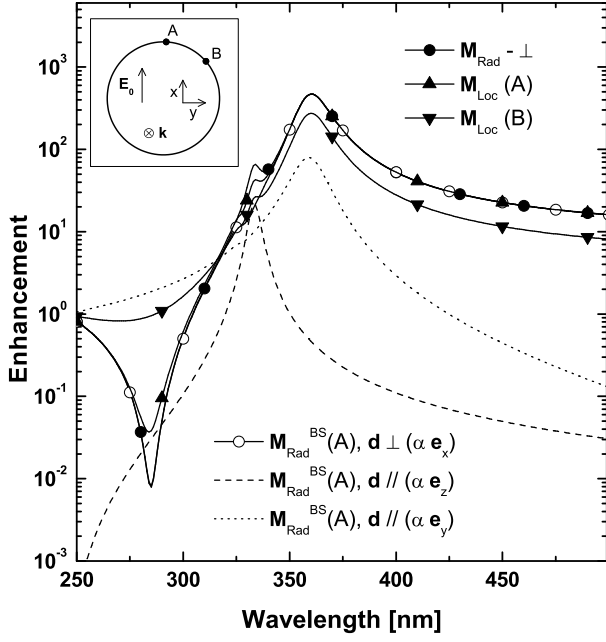


FIG. 4: Example of calculations using the ORT approach for a silver sphere of radius $a = 25$ nm and a dipole situated at $d = 1$ nm from the surface at point A or B (see inset). The radiative enhancement M_{Rad} for a perpendicular dipole and the local field enhancement $|E|^2/|E_0|^2$ at A and B are shown for comparison. The angle dependent radiative enhancement is calculated for the backscattering direction (along $-\mathbf{k}$) for a dipole at A aligned along either \mathbf{e}_x (perpendicular), or \mathbf{e}_z or \mathbf{e}_y (parallel). This requires to calculate the field at A for two plane wave problems, with polarization along x and y . For the perpendicular dipole, $M_{\text{Rad}}^{\text{BS}}$ is indistinguishable from $M_{\text{Loc}}(\text{A})$ and M_{Rad} . For other dipole orientations, it is clear that $M_{\text{Rad}}^{\text{BS}}$ can be very different from M_{Loc} .

(non-radiative) decay paths can exist in a molecule, even in free-space. This intrinsic decay is characterized by a rate $\Gamma_{\text{NR}}^{\text{int}}$. For an excited electron, there is competition between these two mechanisms. In free-space, we assume $\Gamma_{\text{Rad}} = \Gamma_0$ and the quantum yields is then

$$Q_0 = \frac{\Gamma_0}{\Gamma_0 + \Gamma_{\text{NR}}^{\text{int}}} \quad (11)$$

Close to a metal surface, there are two effects that will affect the quantum yield: (i) the radiative decay rate Γ_{Rad} is modified by a factor M_{Rad} , and (ii) there is an additional non-radiative path corresponding to emission into dissipative modes in the metal, with rate $\Gamma_{\text{NR}} = (M_{\text{Tot}} - M_{\text{Rad}})\Gamma_0$. We can rewrite the modified quantum yield as:

$$Q = \frac{\Gamma_{\text{Rad}}}{\Gamma_{\text{Rad}} + \Gamma_{\text{NR}} + \Gamma_{\text{NR}}^{\text{int}}} \quad (12)$$

Using the notations of the previous section and the expression for Q_0 , this can be expressed as

$$Q = \frac{M_{\text{Rad}}}{M_{\text{Tot}} + Q_0^{-1} - 1} \quad (13)$$

At short distances from the metal surface (< 10 nm), M_{Tot} is typically much larger than 1. For a typical fluorophore with a reasonable quantum yield, M_{Tot} will completely dominate the expression in the denominator. The modified quantum yield becomes entirely governed by the interaction with the metal, and *all fluorophores should therefore exhibit the same quantum yield*. This aspect will be discussed further in the context of SEF.

III. SERS CROSS-SECTIONS

A. Scattering processes

Scattering processes (elastic or inelastic) are, in many ways, similar to SE. Excluding stimulation, the scattering involves the ‘spontaneous’ creation of a photon in a mode that was empty. One expects a modification of the scattering cross-section in a similar way as SE rates are modified by the environment. As pointed out in the introduction, the difference between these two processes lies in the initial state: (i) excited atom with no photon for SE and (ii) ground state with one incident photon for scattering. In the classical description of scattering, one can formally distinguish between excitation and re-emission (even though scattering is intrinsically one single process). Using the concept of polarizability, α , (for example Raman or Rayleigh polarizabilities), the excitation part is described by the creation of an induced dipole $\mathbf{d} = \alpha \mathbf{E}_{\text{Loc}}$, where \mathbf{E}_{Loc} is the electric field at the scatterer position. The re-emission problem of this dipole \mathbf{d} can then be treated using the same tools as that developed in Sec. II.

There is, however, a fundamental difference in the physical interpretation of the enhancement factors. $M_{\text{Tot}} = P_{\text{Tot}}/P_0$ characterizes the ability for the environment to extract energy from the dipole, as compared to free-space. For SE, this corresponds to a modification in the total decay rate of the emitter. For scattering, because the process (excitation+re-emission) is instantaneous, this corresponds to a modification of the cross-section. We define here the *total* scattering cross-section as

$$\sigma_{\text{Tot}} = P_{\text{Tot}}/S_0, \quad (14)$$

where

$$S_0 = \epsilon_0 c |E_0|^2 / 2 \quad (15)$$

is the incident flux of the excitation wave (power per unit area), and P_{Tot} is the total power extracted from the induced dipole, as in Sec. II. The standard definition of scattering cross-section [25] corresponds to the *radiative* scattering cross-section:

$$\sigma_{\text{Rad}} = \frac{P_{\text{Rad}}}{S_0}, \quad (16)$$

and similarly, the *differential radiative* scattering cross-section:

$$\frac{d\sigma_{\text{Rad}}}{d\Omega}(\theta, \phi) = \frac{P_{\text{Rad}}(\theta, \phi)}{S_0}. \quad (17)$$

We emphasize here the importance of distinguishing between σ_{Rad} and σ_{Tot} . The difference is similar to the situation in SE between total and radiative decay rates. σ_{Rad} corresponds to the radiated scattered field which can be measured experimentally in the far-field. σ_{Tot} includes σ_{Rad} , but in addition accounts for non-radiative scattering events. These events are not observable in the far-field, but they are indeed experienced by the scatterer. For Raman scattering, it corresponds therefore to the creation of a phonon, and to the emission of a Stokes shifted photon, even if this photon is then absorbed by the environment and not detectable in the far field. This will be important later when discussing vibrational pumping in SERS. This is a similar situation as in modified SE, where an increase in the total decay can be experienced by the emitter (and measured in time-resolved measurements), despite the fact that only radiative enhancement is measured in the far-field.

In Raman scattering, the scatterer is excited at a frequency ω_L , but the induced dipole oscillates at a different frequency ω_R . The difference in energy corresponds to the creation (Stokes process) or destruction (Anti-Stokes process) of a phonon (or vibration). The previous arguments can be easily adapted to the presence of two different frequencies, one for excitation (ω_L), and one for re-emission (ω_R). This enables us to address specifically in the following the SERS-EM enhancement in the context of SE.

B. Local field enhancement factor

In the presence of a dielectric or metallic environment, the field \mathbf{E}_{Loc} at the scatterer position is usually different to the incident field \mathbf{E}_0 . Under certain conditions, in particular close to metallic surfaces, it is well known that the local field intensity at the surface can be much larger than that of the incident field, leading to a *local field enhancement factor* $M_{\text{Loc}}(\omega_L)$. This factor is present for all linear optical processes, such as absorption or scattering. For Raman scattering, it is related to the excitation of the Raman dipole and will depend on the exact Raman tensor of the probe. We only consider here two simple and common cases. For an isotropic Raman tensor, the induced Raman dipole is simply $\mathbf{d} = \alpha\mathbf{E}$, and

$$M_{\text{Loc}} = |\mathbf{E}_{\text{Loc}}|^2/|E_0|^2, \quad (18)$$

For a uni-axial tensor, with a fixed axis along \mathbf{e}_d , the induced dipole is then $\mathbf{d} = \alpha(\mathbf{e}_d \cdot \mathbf{E})\mathbf{e}_d$ and

$$M_{\text{Loc}} = |\mathbf{e}_d \cdot \mathbf{E}_{\text{Loc}}|^2/|\mathbf{e}_d \cdot \mathbf{E}_0|^2. \quad (19)$$

This enhancement has been studied for many geometries using various approximations. Large values of M_{Loc}

are associated with localized surface plasmon resonances at certain wavelengths. They are also typically highly localized, i.e. at the junction of two closely spaced nanoparticles. We showed in Sec. IID that these resonances are closely related to the radiative SP resonances observed for M_{Rad} . M_{Loc} can be estimated to be $\sim 100 - 1000$ at the surface of an Ag colloid at the plasmon resonance energy. Larger values ($10^5 - 10^6$) have been predicted at the junction of two particles, or at sharp corners. For interacting particles the collective resonance is also red-shifted.

C. SE approach to SERS cross sections

SERS corresponds to Raman scattering in close proximity to metallic surfaces, in particular, silver (Ag) and gold (Au). Under the right conditions, a large enhancement is observed in the Raman signal, with apparent cross-sections being as large as 10^{15} times larger than the normal cross-section. The local field enhancement factor M_{Loc} can be as large as $10^5 - 10^6$, but such values are still too small to explain the large reported SERS cross sections. The problem is that M_{Loc} describes well the enhancement associated with the excitation of the molecule, but not the re-emission process. The most common assumption in SERS is that $\sigma \propto M_{\text{Loc}}(\omega_L)M_{\text{Loc}}(\omega_R)$, where $M_{\text{Loc}}(\omega_R)$ is used to model the enhancement associated with re-emission. This is the so-called $|E|^4$ -enhancement and enables to explain easily values up to 10^{12} . However, this approach has not been carefully justified to the best of our knowledge. A few old studies use a proper description of the dipolar emission in the vicinity of metal surfaces, but analytical results are possible only for a single (very small) spheres, where a relation of the type $M_{\text{Loc}}(\omega_L)M_{\text{Loc}}(\omega_R)$ is obtained [32, 33]. The first factor corresponds to excitation while the second comes from the field emitted by the dipole and scattered by the sphere. The optical reciprocity theorem has been cited as a possible general justification of this factor [17] without further details.

The treatment of SERS in the framework of modified SE modification in fact shows that the SERS radiative cross-section enhancement should be derived from Eq. (16):

$$\frac{\sigma_{\text{Rad}}^{\text{SERS}}}{\sigma_0} = M_{\text{Loc}}(\omega_L)M_{\text{Rad}}(\omega_R) \quad (20)$$

This seems in stark contrast with the standard $|E|^4$ approach. The difference stems in the second (re-emission) term: $M_{\text{Rad}}(\omega_R)$, instead of $M_{\text{Loc}}(\omega_R)$, which can be calculated using the tools of Sec. II. These two terms have *a priori* nothing in common. The only relation is through the orientation of the Raman dipole, which is determined by the excitation and can affect the value of $M_{\text{Rad}}(\omega_R)$. However, we will now show using the optical reciprocity theorem that the two approaches can be equivalent under certain conditions. This enables, accordingly, a rigorous

justification of the $|E|^4$ factor and defines precisely its conditions of validity.

D. Generalization of the $|E|^4$ factor

In Sec. IID, we used the ORT to give an alternative expression for the radiative enhancement. The angle-dependent radiative enhancement $M_{\text{Rad}}(\theta, \phi)$ was derived from the solution of two plane wave excitation (PWE) problems. The expression obtained in Eq. (10) resembles that of M_{Loc} in Eq. (19), and is the basis for the justification and generalization of the $|E|^4$ factor. However, because it applies to angle-dependent radiative enhancement, an integration is required for the total radiative enhancement and would lead to:

$$\frac{\sigma_{\text{Rad}}^{\text{SERS}}}{\sigma_0} = M_{\text{Loc}}(\omega_L) \times \int \left[\frac{|\mathbf{e}_d \cdot \mathbf{E}^{\text{PW}-\theta}(\omega_R)|^2}{|E_0|^2} + \frac{|\mathbf{e}_d \cdot \mathbf{E}^{\text{PW}-\phi}(\omega_R)|^2}{|E_0|^2} \right] d\Omega, \quad (21)$$

where \mathbf{e}_d is the orientation of the Raman dipole defined by the Raman tensor and the local field polarization. This expression, although fairly general, has usually no interest in practise because of its complexity. It would indeed require to solve PWE problems for plane waves incident from all possible directions (θ, ϕ) .

However, in most experimental situations, the SERS signal is detected in the far field in only one given direction (θ_d, ϕ_d) . The excitation and detection directions depend on the specific scattering configuration and usually correspond to a small solid angle defined by the numerical aperture of the collecting optics. The physical quantity relevant to the problem is therefore the differential radiative SERS cross-section in the detection direction, σ_{Rad}^d . Using Eq. (10), the SERS enhancement factor in this direction is then given by

$$\frac{\sigma_{\text{Rad}}^d}{\sigma_0^d} = M_{\text{Loc}}(\omega_L) M_{\text{Rad}}(\theta_d, \phi_d, \omega_R) \quad (22)$$

For simplicity, we will focus on the most common SERS setup, namely the back-scattering (BS) configuration, where excitation and detection are along the same direction, say (Oz). We also assume that the incident wave is a plane wave polarized along (Ox). As before, the use of the ORT requires to find the solution of two plane wave problems, with polarization along (Ox) and (Oy). We denote \mathbf{E}^{PX} and \mathbf{E}^{PY} the electric fields at the scatterer position for the solution of these two problems. We can then write the BS radiative SERS enhancement factor as

$$\frac{\sigma_{\text{Rad}}^{\text{BS}}}{\sigma_0^{\text{BS}}} = M_{\text{Loc}}(\omega_L) \left[\frac{|\mathbf{e}_d \cdot \mathbf{E}^{\text{PX}}(\omega_R)|^2}{|E_0|^2} + \frac{|\mathbf{e}_d \cdot \mathbf{E}^{\text{PY}}(\omega_R)|^2}{|E_0|^2} \right], \quad (23)$$

which has some similarities with the conventional $|E|^4$ factor. However, the standard $|E|^4$ factor, which would be here proportional to $|E^{\text{PX}}(\omega_L)|^2 |E^{\text{PX}}(\omega_R)|^2$, in fact

requires the solution of only one plane wave problem, with polarization along (Ox). Since PWE problems along (Ox) and (Oy) are two independent EM problems, one concludes that there must be some information missing in the $|E|^4$ approach, which is therefore at best an approximation.

The exact form of this expression can be further simplified by considering specific Raman tensors for the probe. For an isotropic Raman tensor, we have $\mathbf{d} = \alpha \mathbf{E}^{\text{PX}}(\omega_L)$ leading to

$$\frac{\sigma_{\text{Rad}}^{\text{BS}}}{\sigma_0^{\text{BS}}} = \frac{|\mathbf{E}^{\text{PX}}(\omega_L)|^2 |\mathbf{E}^{\text{PX}}(\omega_R)|^2}{|E_0|^4} + \frac{|\mathbf{E}^{\text{PX}}(\omega_L) \cdot \mathbf{E}^{\text{PY}}(\omega_R)|^2}{|E_0|^4} \quad (24)$$

For the common case of a uniaxial Raman tensor, the induced Raman dipole is $\mathbf{d} = \alpha (\mathbf{E}^{\text{PX}} \cdot \mathbf{e}_d) \mathbf{e}_d$, where \mathbf{e}_d is fixed by the orientation of the molecule. The SERS enhancement is then

$$\frac{\sigma_{\text{Rad}}^{\text{BS}}}{\sigma_0^{\text{BS}}} = \frac{|\mathbf{e}_d \cdot \mathbf{E}^{\text{PX}}(\omega_L)|^2 |\mathbf{e}_d \cdot \mathbf{E}^{\text{PX}}(\omega_R)|^2}{|\mathbf{e}_d \cdot \mathbf{E}_0|^2 |E_0|^2} + \frac{|\mathbf{e}_d \cdot \mathbf{E}^{\text{PX}}(\omega_L)|^2 |\mathbf{e}_d \cdot \mathbf{E}^{\text{PY}}(\omega_R)|^2}{|\mathbf{e}_d \cdot \mathbf{E}_0|^2 |E_0|^2} \quad (25)$$

From the derivation of Eq. (10), one actually sees that the first term in the above expressions corresponds to detection with a polarizer along (Ox), parallel to excitation, while the second is that for a polarizer along (Oy), perpendicular to excitation. The first term is equal to the conventional $|E|^4$ factor. We conclude that this factor can be exact, for example if all the following conditions are met: (i) plane wave excitation, (ii) back-scattering configuration, (iii) polarized detection parallel to excitation, (iv) isotropic or uniaxial Raman tensor. The reason for the first condition is actually quite natural. An emitting dipole cannot distinguish the type of excitation being used. Therefore, the re-emission part is always identical, say for plane waves or Gaussian beams. However, the local field enhancement can change from one type of excitation to another, and the $|E|^4$ approach cannot be true for both. If condition (iii) is not met, for example for non-polarized detection, the $|E|^4$ factor should be in most cases a good approximation, at least for the order of magnitude of the enhancement. However, to study depolarization effects, the standard $|E|^4$ factor is not adequate and the full treatment given above is necessary. Similarly, for other scattering configurations, for example at 90 degrees, the standard $|E|^4$ can lead to erroneous conclusions. This emphasizes one important conclusion of this study often overlooked in the past: accurate SERS enhancement calculations are only possible if the Raman tensor of the probe and the scattering configuration are clearly specified.

E. SERS depolarization ratios and the $|E|^4$ factor

One clear illustration of the failure of the $|E|^4$ factor is in the calculation of SERS depolarization ratios. We here focus on the simplest canonical example of a metallic silver sphere covered by a continuous distribution of probe molecules on its surface. Simple analytical expressions could be obtained in the electrostatics approximation, but we give here exact results, calculated using Mie theory [19, 21]. Two situations are considered: (i) molecules with an isotropic Raman tensor, and (ii) molecules with a uni-axial Raman tensor. In the second case, the axis needs to be specified, and we assume that for each molecule it is fixed and perpendicular to surface of the sphere (this corresponds to a fixed adsorption geometry). Choosing the back-scattering geometry along direction (Oz), excitation is polarized along (Ox) and detected with polarizer along (Ox) (parallel) or (Oy) (perpendicular). The parallel and perpendicular intensities are evaluated by integrating the intensities on the sphere surface, to account for the contribution from all molecules. According to the previous section, the depolarization ratio $R = I_{\perp}/I_{\parallel}$ for the isotropic case is given by:

$$R^{\text{ORT}} = \frac{\int |\mathbf{E}^{\text{PX}}(\omega_L) \cdot \mathbf{E}^{\text{PY}}(\omega_R)|^2}{\int |\mathbf{E}^{\text{PX}}(\omega_L)|^2 |\mathbf{E}^{\text{PX}}(\omega_R)|^2}. \quad (26)$$

Using the conventional $|E|^4$ factor, combined with standard techniques of depolarization scattering, one would obtain:

$$R^{\text{E4}} = \frac{\int |\mathbf{E}^{\text{PX}}(\omega_L)|^2 |\mathbf{e}_y \cdot \mathbf{E}^{\text{PX}}(\omega_R)|^2}{\int |\mathbf{E}^{\text{PX}}(\omega_L)|^2 |\mathbf{e}_x \cdot \mathbf{E}^{\text{PX}}(\omega_R)|^2}. \quad (27)$$

For the perpendicular uniaxial case, these relations are:

$$R^{\text{ORT}} = \frac{\int |\mathbf{E}^{\text{PX}}(\omega_L) \cdot \mathbf{e}_r|^2 |\mathbf{E}^{\text{PY}}(\omega_R) \cdot \mathbf{e}_r|^2}{\int |\mathbf{E}^{\text{PX}}(\omega_L) \cdot \mathbf{e}_r|^2 |\mathbf{E}^{\text{PX}}(\omega_R) \cdot \mathbf{e}_r|^2}, \quad (28)$$

and

$$R^{\text{E4}} = \frac{\int |\mathbf{E}^{\text{PX}}(\omega_L) \cdot \mathbf{e}_r|^2 |\mathbf{E}^{\text{PX}}(\omega_R) \cdot \mathbf{e}_r|^2 |\mathbf{e}_y \cdot \mathbf{e}_r|^2}{\int |\mathbf{E}^{\text{PX}}(\omega_L) \cdot \mathbf{e}_r|^2 |\mathbf{E}^{\text{PX}}(\omega_R) \cdot \mathbf{e}_r|^2 |\mathbf{e}_x \cdot \mathbf{e}_r|^2}. \quad (29)$$

For simplicity, we also make the common assumption of a negligible Raman shift: $\omega_L \approx \omega_R$. Despite the apparent similarities between the ORT and $|E|^4$ expressions, they are actually very different. Note in particular the difference in the numerators. In the first case, one needs to solve a second PWE problem with polarization along (Oy) to obtain \mathbf{E}^{PY} , while in the second, one PWE problem is sufficient and the solution is simply projected onto \mathbf{e}_y . This conceptual difference leads to drastically different predictions, as shown in Fig. 5, where the two models are plotted as a function of wavelength. In the uniaxial case, the $|E|^4$ approach predicts a constant (wavelength independent) ratio of 1/5, whereas a ratio of 1/3 is predicted from the ORT approach. For

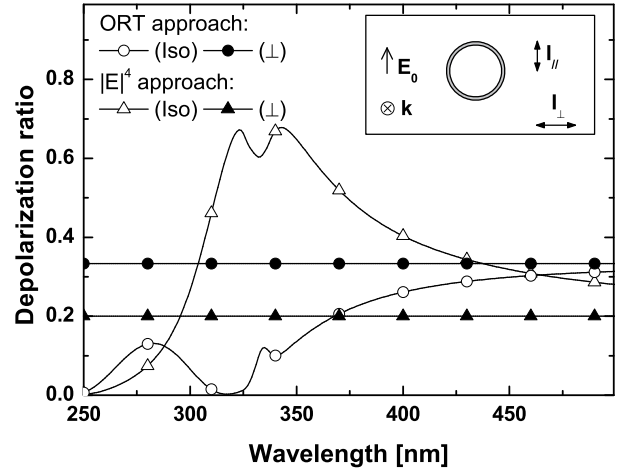


FIG. 5: Comparison of the predictions from the standard $|E|^4$ approach, with that of modified SE using the ORT. The SERS depolarization ratio $R = I_{\perp}/I_{\parallel}$ is shown as a function of wavelength for a continuous distribution of probe molecules on the surface of a silver sphere of radius $a = 25$ nm. Two Raman tensors are considered: isotropic (Iso), or uniaxial with the main axis perpendicular to the sphere surface (\perp). This clearly illustrates the failure of the $|E|^4$ approximation under certain conditions.

the isotropic tensor, the behavior at the surface plasmon resonance of the sphere is simply the opposite. The standard $|E|^4$ approach predicts a ratio increasing to ≈ 0.7 , while the generalized approach predicts a decrease close to 0. Such discrepancies are also likely for depolarization ratios calculations in more complex geometries; a subject which will be explored in further detail in a forthcoming publication.

F. Image dipole enhancement

Before discussing these results any further, we would like to mention an additional enhancement mechanism, which we have neglected in the previous considerations, namely: the image dipole enhancement. This does not apply to SE, but is present for many other processes, in particular absorption and scattering. This mechanism has been discussed in the past [34, 35, 36], but has since then been overlooked. It actually appears naturally when considering SERS in the framework of modified spontaneous emission. For SE, the self-reaction field modifies the ability of the dipole to radiate energy. Although the ‘re-emission’ enhancement in SERS follows the physics of modified SE we have to consider an additional ingredient: in SE the dipole is already in an ‘excited’ state with a fixed dipole amplitude, whereas for scattering, the dipole is constantly driven by an external field. A constant source of energy is then readily available from the laser. The self-reaction field can therefore, in addition, oppose or amplify the dipole amplitude (fixed by the dipole moment in SE). *This leads to the concept of*

effective polarizability. We assume in this section for simplicity that the molecular polarizability and self-reaction tensor \mathbf{G}_r are isotropic. The dipole is driven by both the external and reflected fields, which leads to a modified polarizability of the form [34, 35, 36]

$$\alpha_m = \alpha_0 (1 - \alpha_0 G_r)^{-1}, \quad (30)$$

which in turn leads to an additional enhancement (or quenching) factor

$$M_{\text{Im}}(\omega) = \frac{|\alpha_m|^2}{|\alpha_0|^2} = \frac{1}{|1 - \alpha_0(\omega)G_r(\omega)|^2}. \quad (31)$$

For a dipole near a metallic plane, the self-reaction field in the electrostatics approximation corresponds to the field created by an image dipole and we have

$$G_r \approx \frac{1}{8\pi\epsilon_0 d^3} \frac{\epsilon_r - 1}{\epsilon_r + 1}, \quad (32)$$

for a dipole perpendicular to the surface (half of this result for a parallel dipole). M_{Im} can therefore be called the image dipole enhancement factor. This factor now involves both the real and imaginary part of G_r .

The same effect applies to SERS through the effective Raman polarizability. This has been studied in the past [34, 35, 36] and leads in the first approximation to an additional enhancement $M_{\text{Im}}(\omega_L)M_{\text{Im}}(\omega_R)$. The image dipole enhancement factors had been proposed in the past to explain SERS enhancements [34, 35, 36] but were then thought to be too small and have not been since then part of the main discussions in the field. One reason is that it has so far been studied mainly for plane metallic surfaces. In Sec. II C, we have shown that for a sphere or more complex structures, radiative enhancements can be large and form a substantial part of M_{Tot} . From Eq. (5), this means that G_r must be strongly affected by the radiative SP resonances. The common electrostatic approximation of the image dipole then fails, and it is possible that image dipole enhancement factors become non-negligible under these conditions. This factor could then play a decisive role in explaining the role of the polarizability of the probe in the total scattering cross section and, in particular, the fact that dyes are the most effective SERS probes in general.

G. Comparison with Surface Enhanced Fluorescence

In many cases, the emission from fluorophores very close to metal surfaces is strongly quenched by large non-radiative energy transfer. However, several recent experiments have evidenced fluorescence enhancements, for example close to Ag or Au surfaces [8, 9]. There still seems to be some debate about the origin of this enhancement and the exact conditions under which it takes place. Many of the arguments and tools developed so far can actually be adapted to the study of Surface Enhanced Fluorescence (SEF), and shed light onto this problem. This

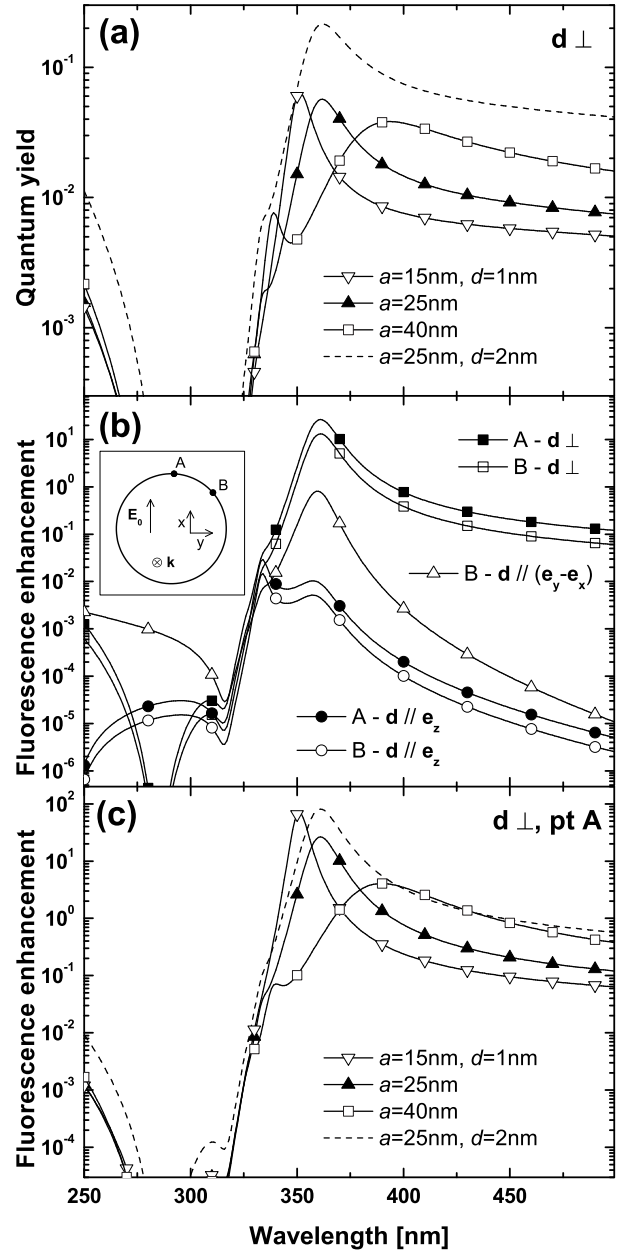


FIG. 6: Surface Enhanced Fluorescence for a fluorophore situated at a distance $d = 1$ or 2 nm from a silver sphere of radii $a = 15, 25,$ and 40 nm. The intrinsic quantum yield, Q_0 is assumed to be 1, but the results are insensitive to Q_0 unless it is extremely small. (a) Modified quantum yield (see Sec. II E). This is in principle not directly observable in SEF, because local field enhancements also play an important role during excitation of the fluorophore. (b) Fluorescence enhancement for dipoles at two different position with various orientations. Note that some configurations always result in quenching and not enhancement. (c) Influence of a and d on the fluorescence enhancement. Enhancements are observed at the surface plasmon resonance of the sphere. Largest enhancements are observed for the smallest sphere and for a dipole slightly away from the surface. Note that for comparison with most experiments, it is necessary to integrate the fluorescence intensity from all points on the surface of the sphere.

is also relevant to the problem of fluorescence quenching under SERS conditions.

Fluorescence is very similar to scattering; it involves absorption of a photon, followed by emission. The same enhancement mechanisms as that derived for SERS are therefore expected. The absorption should be subject to the local field enhancements, and the emission is simply SE and should follow the same enhancements. The image dipole enhancement should also be present for absorption, but we neglect this aspect here for simplicity. *The crucial difference is that SERS is instantaneous while fluorescence is a multi-step process.* This means that both enhancements (local field and SE type) contribute to the SERS cross-section. For fluorescence, the local field enhancement does also lead to a modification of the absorption cross-section, but the SE-type enhancements only lead to modification of the decay rates (radiative and non-radiative). To put it differently, once a photon is absorbed and excites an electron in fluorescence, enhancements cannot lead to more energy being extracted from this electron, but only to energy being extracted faster.

To be more specific, we consider a fluorophore as in Sec. II E, with an absorption cross-section k_0 , a radiative rate Γ_0 , and a quantum yield Q_0 . We neglect here the shift between excitation and fluorescence energies. Under a given excitation, the photon flux is $n_0 \propto |E_0|^2$ and the power radiated by fluorescence in free-space is (in number of photons per unit time):

$$P_0^{\text{Fluo}} = k_0 n_0 Q_0 \quad (33)$$

We have assumed here that the power is small enough to avoid saturation effects in the excited state. In this expression, $k_0 n_0$ is the number of photons absorbed per unit time. For each excited electron, the probability of being emitted radiatively is simply Q_0 . If the fluorophore is now close to a metal surface, we can use the same expression, with the modified quantum yield Q given by Eq. (13). The absorption rate is also modified because the field intensity at the fluorophore position is now $M_{\text{Loc}}|E_0|^2$. The fluorescence enhancement (or quenching) is then:

$$\frac{P^{\text{SEF}}}{P_0^{\text{Fluo}}} = M_{\text{Loc}} \frac{M_{\text{Rad}}}{M_{\text{Tot}} + Q_0^{-1} - 1} \quad (34)$$

Moreover, in many cases, $Q_0^{-1} - 1$ can be neglected. This expression clearly identifies the sources of enhancement or quenching. There are in fact two competing mechanisms: (i) the first term, the local field enhancement M_{Loc} , which in most situations of interest is larger or much larger than 1, and leads to enhanced fluorescence, and (ii) the second term which is the radiative efficiency of the emitter in electromagnetic interaction with the metal. This term is smaller (and sometimes much smaller) than 1 and corresponds to quenching. Quenching and enhancement of fluorescence are therefore two sides of the same problem. The various reports on quenching and enhancement of fluorescence are nothing

but different situations where either the first or second terms in Eq. (34) dominates with respect to the other.

These aspects are illustrated in Fig. 6, for the case of a silver sphere, where various cases of dipole orientation, sphere radius, and distance from the surface are considered. These plots show that the conditions for fluorescence enhancements depend on many parameters, and are in general not trivial to determine. There are however a few general observations:

- The region of fluorescence enhancement is relatively small compared to that of fluorescence quenching. It requires an efficient coupling to the radiative SP resonance of the sphere. This point had already been emphasized in Ref. [8].
- The largest enhancement can in principle be obtained for the smallest sphere radii (see Fig. 6(c)). This is the opposite conclusion to that reached in Ref. [8], based on the idea that scattering is more dominant compared to absorption for the largest sphere. This re-emphasizes the fact that these effects are not simple and require a careful consideration of all enhancement and quenching factors.
- Increasing slightly the distance d between emitter and surface in general leads to higher fluorescence enhancements. This is because the local field enhancement does not change much at short distances, while non-radiative decay decreases sharply with d . For dyes adsorbed on the surface, varying d is not straightforward. However, for fluorescing quantum dots, d should depend on the size of the quantum dot, and a careful tuning could possibly lead to large fluorescence enhancements [9].

IV. DISCUSSION

In view of the previous description of SERS within the framework of modified spontaneous emission, we can summarize the electromagnetic enhancement of the radiative SERS cross section as

$$\frac{\sigma_{\text{Rad}}^{\text{SERS}}}{\sigma_0} = M_{\text{Im}}(\omega_L) M_{\text{Loc}}(\omega_L) M_{\text{Rad}}(\omega_R) M_{\text{Im}}(\omega_R), \quad (35)$$

where M_{Im} is given by Eq. (31), M_{Loc} is given by Eq. (18) (or Eq. (19) depending on the Raman tensor), M_{Rad} is given by Eq. (10) (for detection along a specific direction), and with all the expressions evaluated at either the laser (ω_L) or the Raman (Stokes or Anti-Stokes) frequencies (ω_R).

The first two terms relate to the excitation part, while the last two to re-emission. Moreover, M_{Rad} is related to M_{Loc} for plane wave excitation using the ORT, in a way defined in the previous sections. We conclude this study by discussing briefly a few aspects of this expression that have been, in our opinion, not fully accounted for in the past.

A. Image dipole enhancement factors

A detailed discussion of this factor requires a full paper in itself. Our numerical simulations (not shown here) indicate that this factor contributes to a $\sim 10^3$ enhancement at most. *It is however important that this factor is the only one in Eq. (35) that involves the linear polarizability of the molecule.* It can therefore be the natural origin for a number of characteristics in SERS. The fact that only dyes exhibit the largest SERS cross section (having large optical polarizabilities in the visible) comes as a natural consequence here. We only mention briefly too that this factor can explain the apparent resonance profile observed in many SERS experiments [15, 37] and can be of additional importance in Surface Enhanced Resonant Raman Scattering (SERRS).

B. Fluorescence quenching and the SERS continuum

We consider here the common case of a dye under SERS conditions. It is well known that fluorescence is strongly quenched when large SERS signals are observed. This should in principle be derived naturally within our framework. However, we have seen that SERS and SEF are in fact subject to the same local field enhancement factor and one could therefore expect the two to be correlated. In fact, combining Eqs. (20) and (34) we see that the SERS and SEF enhancement factors are directly related through $M_{\text{SERS}} = M_{\text{Tot}}M_{\text{SEF}}$. In a typical SERS situation, M_{Tot} can be very large, say 10^5 , and SERS enhancements are therefore much larger than fluorescence enhancements. This factor is still however much too small to offset the intrinsic larger efficiencies of fluorescence processes as compared to Raman, which typically differ by factors of $\sim 10^{10} - 10^{15}$. We would therefore expect fluorescence to be enhanced less than Raman but still remain strong compared to Raman under SERS conditions.

To understand this apparent paradox we need to re-examine the situation of SEF under conditions of very high enhancement, where the total decay rate $M_{\text{Tot}}\Gamma_0$ is many orders of magnitude larger than usual. When decay rates become comparable or smaller than the typical energy relaxation times, then the electron dynamics in the relaxation pathways is strongly modified. Very close to a noble metal surface M_{Tot} can be $\sim 10^5$ or higher. For a typical SE lifetime of a few ns, the modified lifetime would only be of the order of a few tens of fs or less, i.e much shorter than typical energy relaxation times in molecules. In this model, this would imply that absorbed photons do not have time to relax and are emitted at the frequency they were absorbed. Standard fluorescence would therefore be quenched and appears as an increase in Rayleigh scattering. Indeed, such enhancements have been reported under SERS conditions, but it is difficult to test whether they are true Rayleigh scat-

tering or strongly modified fluorescence. Pushing this argument further, for the shortest decay times, the uncertainty principle would also imply that energy is not well defined in the intermediate levels of the relaxation path with a typical spread of 1600 cm^{-1} for times of 10 fs. The whole process would qualitatively result in a very broad emission from all possible intermediate virtual states. We propose that this could be the origin of the strongly debated SERS continuum, which is observed in many SERS experiments. A proper treatment of such extreme conditions however requires a full quantum mechanical study of absorption-relaxation-emission similar to that of Ref. [17].

C. Non-radiative effects in SERS

Finally, this approach also highlights the importance of non-radiative effects in SERS. In fluorescence, non-radiative effects manifest themselves as a reduced quantum yield, because of the competition between radiative and non-radiative decays. In SERS, because scattering is instantaneous, there is not such a competition, and radiative and non-radiative emission can occur independently of each other. Similarly to SE, we can define a total (radiative+non-radiative) SERS cross-section (we ignore here M_{Im}).

$$\frac{\sigma_{\text{Tot}}^{\text{SERS}}}{\sigma_0} = M_{\text{Loc}}(\omega_L)M_{\text{Tot}}(\omega_R) \quad (36)$$

Under SERS conditions, this cross-section can be much larger than the observable radiative SERS cross-section, as given in Eqs. (20), (22), or (35). The difference corresponds to Raman processes resulting in emission of a Raman photon in the non-radiative modes of the metal. These Raman photons are obviously non-observable in the far-field, but they do correspond to a real Raman event, and therefore to the creation or destruction of a vibration in the molecule. This total SERS cross-section is therefore the one that is relevant when studying phonon population dynamics, in particular effects such as vibrational pumping [38, 39]. This could make the much debated hypothesis of vibrational pumping more likely, since the cross-section for phonon pumping could actually be much larger than that inferred for the radiative SERS cross-sections in the far-field.

D. Conclusion

In closing, we have presented a consistent formulation of cross-section enhancements in SERS and fluorescence within the framework of modified spontaneous emission. The local field enhancements, and the competition between radiative and non-radiative decays have been shown to have different consequences for fluorescence and for scattering. This description provides a relatively simple way of designing and modelling metallic

nano-structures for specific applications, either in SEF, or in SERS. The model also highlights the shortcomings of the usual $|E|^4$ -proportionality in the SERS cross section, often assumed in the literature, and provides a direct recipe for its calculation based on classical electromagnetic theory, self-reaction effects, and the optical reciprocity theorem. This approach could explain some

of the longstanding puzzles in SERS like the presence of a SERS continuum, the increase in Rayleigh scattering simultaneous with SERS, and the peculiar ability of dyes to be very efficient probes. Full details of calculations using this EM SERS cross section with applications to other more complex and relevant geometries will be reported elsewhere.

-
- [1] E. M. Purcell, Phys. Rev. **69**,681 (1946).
- [2] K. H. Drexhage, H. Kuhn, F. P. Scäfer, Ber. Bunsenges. Phys. Chem. **72**, 329 (1968).
- [3] P. Goy, J. Raymond, M. Gross, and S. Haroche, Phys. Rev. Lett. **50**, 1903 (1983).
- [4] R. R. Chance, A. Prock, and R. Silbey, Adv. Chem. Phys. **37**, 1 (1978).
- [5] H. Metiu, Progress. Surf. Sci. **17**, 153 (1984).
- [6] G. W. Ford and W. H. Weber, Phys. Rep. **113**, 195 (1984); and references therein.
- [7] E. Dulkeith, A. C. Morteani, T. Niedereichholz, T. A. Klar, J. Feldmann, S. A. Levi, F. C. J. M. van Veggel, D. N. Reinhoudt, M. Möller, and D. I. Gittins, Phys. Rev. Lett. **89**, 203002 (2002).
- [8] J. R. Lakowicz, Analytical Biochem. **337**, 171 (2005).
- [9] J.-H. Song, T. Atay, S. Shi, H. Urabe, and A. V. Nurmikko, Nano Lett. **5**, 1557 (2005).
- [10] M. Moskovits, Rev. Mod. Phys. **57**, 783 (1985).
- [11] K. Kneipp, Y. Wang, H. Kneipp, L. T. Perelman, I. Itzkan, R. R. Dasari, and M. S. Feld, Phys. Rev. Lett. **78**, 1667 (1997).
- [12] S. Nie and S. R. Emory, Science **275**, 1102 (1997).
- [13] T. Vo-Dinh, D. L. Stokes, G. D. Griffin, M. Volkan, U. J. Kim, and M. I. Simon, J. Raman Spectrosc. **30**, 785 (1999).
- [14] K. Kneipp, H. Kneipp, I. Itzkan, R. R. Dasari, and M. S. Feld, J. Phys.: Cond. Matt. **14**, R597 (2002).
- [15] E. C. Le Ru, M. Dalley, and P. G. Etchegoin, Curr. Appl. Phys. (in press).
- [16] J. Jiang, K. Bosnick, M. Maillard, and L. Brus, J. Phys. Chem. B **107**, 9964 (2003).
- [17] H. Xu, X.-H. Wang, M. P. Persson, H. Q. Xu, M. Käll, and P. Johansson, Phys. Rev. Lett. **93**, 243002 (2004).
- [18] L. A. Blanco and F. J. García de Abajo, Phys. Rev. B **69**, 205414 (2004).
- [19] G. Mie, Ann. Phys. **25**, 377 (1908).
- [20] L. Landau, E. Lifchitz, and L. Pitaevskii, *Electromagnet-ics of Continuous Media* (Pergamon, Oxford, 1984).
- [21] C. F. Bohren and D. R. Huffman, *Absorption and Scattering of Light by Small Particles* (Wiley, New York, 1983).
- [22] H. Chew, J. Chem. Phys. **87**, 1355 (1987).
- [23] S. M. Barnett, B. Huttner, and R. Loudon, Phys. Rev. Lett. **68**, 3698 (1992).
- [24] C. Cohen-Tannoudji, J. Dupont-Roc, and G. Grynberg, *Photons and Atoms* (Wiley, New York, 1997), p. 70.
- [25] J. D. Jackson, *Classical Electrodynamics* (Wiley, New York, 1998).
- [26] H. Morawitz, Phys. Rev. **187**, 1792 (1969).
- [27] H. Kuhn, J. Chem. Phys. **53**, 101 (1970).
- [28] H. Morawitz and M. R. Philpott, Phys. Rev. B **10**, 4863 (1974).
- [29] R. Fuchs and R. G. Barrera, Phys. Rev. B **24**, 2940 (1981).
- [30] H. F. Arnoldus and T. F. George, Phys. Rev. A **37**, 761 (1988).
- [31] J.Y. Courtois, J.M. Courty, J. C. Mertz, Phys. Rev. A **53**, 1862 (1996).
- [32] M. Kerker, D.-S. Wang, and H. Chew, Appl. Optics **19**, 4159 (1980).
- [33] R. Rojas V and F. Claro, J. Chem. Phys. **98**, 998 (1993).
- [34] F. W. King, R. P. Van Duyne, and G. C. Schatz, J. Chem. Phys. **69**, 4472 (1978).
- [35] S. Efrima and H. Metiu, J. Chem. Phys. **70**, 1602 (1979).
- [36] W. H. Weber and G. W. Ford, Phys. Rev. Lett. **44**, 1774 (1980).
- [37] R. C. Maher, J. Hou, L. F. Cohen, E. C. Le Ru, J. M. Hadfield, J. E. Harvey, P. G. Etchegoin, F. M. Liu, M. Green, R. J. C. Brown, M. J. T. Milton, J. Chem. Phys., in press.
- [38] K. Kneipp, Y. Wang, H. Kneipp, I. Itzkan, R. R. Dasari, and M. S. Feld, Phys. Rev. Lett. **76**, 2444 (1996).
- [39] E. C. Le Ru and P. G. Etchegoin, Faraday Discuss. **132**, in press.